Available online at www.sciencedirect.com
ScienceDirect
Journal of Catalysis 255 (2008) 304–312
JOURNAL OF CATALYSIS
www.elsevier.com/locate/jcat

On the different roles of isocyanate and cyanide species in propene-SCR over silver/alumina

Stefanie Tamm *, Hanna Härelind Ingelsten, Anders E.C. Palmqvist

Applied Surface Chemistry and Competence Centre for Catalysis, Chalmers University of Technology, SE-412 96 Göteborg, Sweden

Received 30 October 2007; revised 20 February 2008; accepted 21 February 2008

Available online 24 March 2008

Abstract

Silver/alumina is one of the most promising catalyst materials for HC-SCR. The reaction mechanism remains incompletely understood, however. Isocyanate species (–NCO) and cyanide species (–CN), important intermediates in the reaction path in HC-SCR, were investigated by gas-phase FTIR and DRIFT spectroscopy in step-response experiments. In accordance with the literature, the corresponding gas-phase species, HNCO and HCN, were always detected at the same time at the different steps of the experiment; however, the accumulation and consumption of surface –NCO and –CN species did not show a similar correlation. Consequently, in conflict with the literature, we propose two parallel, independent reaction pathways for –NCO and –CN species. In one of these reaction pathways, surface nitrates react with C-containing surface species either directly to –NCO or via R–NO_2 species. In the other pathway, C-containing surface species react with gas-phase NO_x or short-lived N-containing surface species to R–NO species and subsequently to –CN species.

Keywords: Silver/alumina; Propene-SCR; Reaction mechanism; NCO; CN; NO_x reduction

1. Introduction

The interest in fuel-efficient engines that run under oxygen excess has grown recently due to two parallel driving forces: the increasing CO_2 concentration in the atmosphere and increasing oil prices caused by an imbalance between oil production and demand. However, in the lean exhaust environment of these fuel-efficient engines, NO_x cannot be reduced efficiently with a conventional three-way catalyst. There are currently three main alternative catalyst concepts for lean NO_x reduction: NO_x traps, ammonia-assisted selective catalytic reduction (ammonia-SCR), and hydrocarbon-assisted selective catalytic reduction (HC-SCR). Of these alternatives, HC-SCR is the least efficient but offers advantages in terms of implementation, engine operation, comfort, cost, and sometimes durability.

Silver/alumina (Ag/Al_2O_3) is currently one of the most promising catalyst materials for HC-SCR. Although much research has been done on the Ag/Al_2O_3 system, the detailed reaction mechanisms involved in NO_x reduction remain incompletely understood. Burch et al. have reviewed the proposed reaction mechanisms for HC-SCR over Ag/Al_2O_3 [1]. Isocyanate species (–NCO), cyanide species (–CN), amines (R–NH_2), and ammonia (NH_3) are widely believed to be key intermediates in N_2 formation. Experiments with –NCO and/or –CN species in the feed or preadsorbed on the catalyst have shown that N_2 can be formed from –NCO and –CN species under different conditions; isocyanate species react with O_2 or a mixture of NO and O_2, forming N_2 over Ag/Al_2O_3 [2–5], whereas –CN species react efficiently only with NO_2, forming N_2. The latter reaction has been studied only over pure alumina and over zeolite-based catalysts [6,7]. In the presence of water, NH_3 is formed from both –NCO and –CN species [5–9]. The reaction route resulting in isocyanates and cyanides remains under debate, however.

On different oxide catalysts, isocyanates and cyanides can be formed from CO and NO through dissociation and recombination of the species [5,10–12]. Sumiya et al. and Shimizu et al. reported that organic N-containing compounds are involved in the formation of –NCO and –CN species over an Ag/Al_2O_3 catalyst under reaction conditions [2,4]. The appearance and reactivity of these organic N-containing compounds

* Corresponding author. Fax: +46 (0) 31 160062.
E-mail address: stamm@chalmers.se (S. Tamm).

0021-9517/$ – see front matter
doi:10.1016/j.jcat.2008.02.019

have been studied in more detail over zeolite-based catalysts and partly confirmed over Ag/Al_2O_3 catalysts. Cant and Liu [7] studied the decomposition of nitromethane (CH_3–NO_2) and formamide (NH_2–CHO) as an alternative for nitrosomethane (CH_3–NO) over a Co-MFI catalyst, and found that HNCO acted as an intermediate in the decomposition of nitromethane. For the decomposition of formamide, HCN was the major product below 250 °C [7]. This is in agreement with the findings of Nanba et al. [9] demonstrating that HNCO is a decomposition product of nitroethylene over H-ferrierite. Although these authors suggested a possible pathway to HCN formation from nitroethylene, they predicted nitrosoethylene as a key intermediate in HCN formation [9].

Nitro-organo compounds, especially nitromethane, also have been investigated for Ag/Al_2O_3 catalysts as intermediate species in the formation of –NCO and –CN [1,13]. For this system, however, –CN species are believed to be a byproduct of [13] or a precursor for [5,14] –NCO formation. He and Yu [15] studied the roles of acetate and enolic species as possible key intermediates in ethanol-SCR and found that –NCO was formed more efficiently from enolic species than from acetate. In the presence of water, less acetate species were found on the catalyst surface, whereas the amount of enolic species seemed relatively stable [15]. Zhang et al. also stressed the importance of enolic species and ascribed the positive effect of H_2 in ethanol-SCR over Ag/Al_2O_3 to promotion of the formation of enolic species [8].

Evidently, isocyanate (–NCO) and cyanide (–CN) species are widely accepted as key intermediates in HC-SCR. However, an investigation of the differences in these species in the reaction paths over Ag/Al_2O_3 and of the different conditions that lead to –NCO and/or –CN formation has not been published to date. Consequently, the objectives of the present study were to gain insight into the role of different nitrogen-containing intermediates (particularly –CN and –NCO species) in propene-SCR over Ag/Al_2O_3, and also to propose an updated reaction mechanism for these species. We performed step-response experiments in a monolith flow reactor connected to a gas-phase Fourier-transformed infrared (FTIR) spectrometer to investigate gas-phase species. In parallel, we carried out similar step-response experiments using a diffuse reflectance infrared Fourier-transform spectroscopy (DRIFTS) in-situ reactor cell to investigate the surface species present on the catalyst.

2. Methods

2.1. Catalyst preparation

The Ag/Al_2O_3 catalyst was prepared in a two-step process. First, silver nanoparticles were prepared in a water-in-oil (w/o) microemulsion as described by Andersson et al. [16]. Under stirring, an aqueous solution of $AgNO_3$ (2 wt% Ag in MilliQ water, VWR International) was added to a mixture of *n*-heptane (Merck) and Brij 30 (Aldrich), forming a microemulsion containing 75 wt% *n*-heptane, 20 wt% Brij 30, and 5 wt% silver solution. Metallic silver particles were formed within the water droplets through a reduction of Ag^+ ions with the ethylene oxide groups of the surfactant. The reaction took approximately 24 h to complete and resulted in a suspension of Ag particles ranging in size from ca. 5 to 100 Å, with a maximum in size distribution at about 40 Å [16]. To this suspension, γ-Al_2O_3 powder (SASOL Puralox SBa-200) was added under stirring. Subsequently, tetrahydrofuran (Riedel de Haën), in a volume three times as large as the suspension, was slowly added to break the microemulsion and facilitate the deposition of the silver particles on Al_2O_3, as described previously [17]. After 4 h, the suspension was filtered, and the solid material was dried in air at ambient temperature, yielding a powder. Finally, the powder was calcined in air at 550 °C for 3 h, giving the Ag/Al_2O_3 catalyst powder. The BET surface area of the powder was 197 m^2/g as determined by N_2 sorption at −196 °C using a Micromeritics ASAP 2010, and the silver content was 2.2 wt% as determined by SEM-EDX (Leo Ultra 55 FEG SEM). For the DRIFTS measurements, the catalyst powder was subjected to no further treatment.

For the flow-reactor experiments, the Ag/Al_2O_3 catalyst powder was wash-coated on a honeycomb-structured cordierite monolith (400 cpsi) at a catalyst powder:binder weight ratio of 80:20 (Disperal Sol P2, Condea), with a total weight of the washcoat corresponding to 20% of the monolith catalyst weight. A more detailed description of the wash-coating can be found elsewhere [18]. The catalyst was finally calcined in air at 550 °C for 2 h. The BET surface area of the monolith catalyst was 42.9 m^2/g as determined by N_2 sorption at −196 °C using a Micromeritics ASAP 2010.

2.2. Flow reactor experiments

A horizontally mounted quartz-tube reactor was used for the catalytic activity tests. The reactor temperature was measured in the gas stream before the catalyst and inside a channel in the center of the monolith. The effluent gases were mixed by a computerized multicomponent gas mixer (Environics 2000). The reactor exhaust gas composition was analyzed by a gas-phase FTIR (mks instruments, MultiGas 2030) and a NO_x detector (Eco Physics, CLD 799 EL ht).

Before each experiment, the catalyst was pretreated in a gas stream of 8% O_2 in Ar at 550 °C for 30 min. Temperature ramps were performed with a feed gas composition of 1000 ppm NO, 500 ppm C_3H_6, and 8% O_2, balanced with Ar between 200 and 550 °C with a ramp rate of 10 K/min. Step-response experiments were carried out at a fixed temperature of 475 °C and a continuous flow of 8% O_2 in Ar. Nitrogen oxide (1000 ppm) and propene (500 ppm) were switched on and off, with each mixture maintained for 15-min periods (see Table 1 for more details). All flow reactor experiments and the pretreatment were performed with a space velocity of 33,400 h^{-1}.

2.3. DRIFTS experiments

The in-situ DRIFTS experiments were carried out in a Bio-Rad FTS 6000 spectrometer equipped with a high-temperature reaction cell (Harrick Scientific, Praying Mantis) with KBr windows. The temperature of the reaction cell was controlled with

Table 1
Feed gas composition during the different steps in the step-response experiments

Step 1	1000 ppm NO		8% O_2
Step 2	1000 ppm NO	500 or 1000 ppm C_3H_6[a]	8% O_2
Step 3		500 or 1000 ppm C_3H_6[a]	8% O_2
Step 4	1000 ppm NO	500 or 1000 ppm C_3H_6[a]	8% O_2
Step 5	1000 ppm NO		8% O_2
Step 6	1000 ppm NO	500 or 1000 ppm C_3H_6[a]	8% O_2

[a] 500 ppm C_3H_6 were used in the flow reactor and 1000 ppm in the DRIFTS cell.

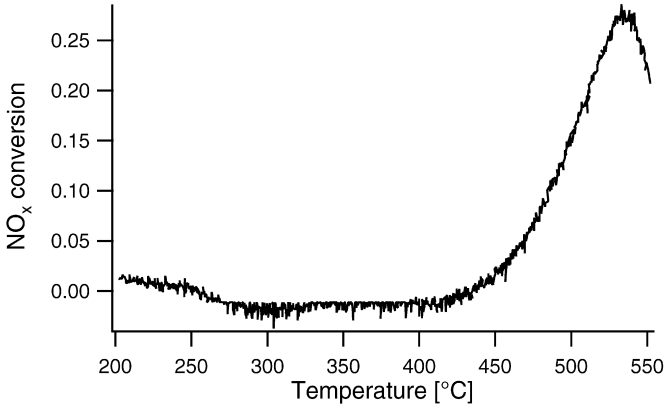

Fig. 1. NO_x conversion as a function of temperature in an effluent mixture of 1000 ppm NO, 500 ppm C_3H_6, and 8% O_2 in Ar.

a K-type thermocouple connected to a Eurotherm 2416. Gases were introduced into the reaction cell via mass flow controllers (Bronkhorst Hi-Tech) and further analyzed after the DRIFTS cell by a mass spectrometer (Balzers QuadStar 420). All of the DRIFTS experiments were carried out at a flow rate of 200 mL/min.

The catalyst was initially pretreated in a flow of 8% O_2 in Ar at 500 °C for 30 min and then flushed with Ar for 15 min. Background spectra (50 scans, resolution 2 cm^{-1}) were obtained before each experiment in an Ar flow at the reaction temperature. The buildup of adsorption bands was followed in the kinetic mode, obtaining 2 scans/min (9 scans/scan) at a resolution of 2 cm^{-1}. Step-response experiments in a continuous flow of 8% O_2 in Ar were performed over Ag/Al_2O_3 at 475 °C with 1000 ppm NO and 1000 ppm C_3H_6 switched on and off (see Table 1 for more details).

3. Results

3.1. Catalytic activity

NO_x conversion of the Ag/Al_2O_3 catalyst was studied in the flow reactor and is plotted as a function of inlet temperature in Fig. 1. Under the conditions used here, a maximum NO_x conversion of 27% was achieved at 535 °C. This maximum activity is comparatively poor for an Ag/Al_2O_3 catalyst; however, the preparation method used left no N- or S-containing residuals on the catalyst surface, which in this study was more important than high activity to avoid interference in the studies of adsorbed surface species. Even though the absolute amounts of adsorbed surface species may have been affected by the degree of NO_x conversion, this does not affect our conclusions, because here we consider only the relative changes of the surface species. Furthermore, the accuracy of the NO_x conversion is somewhat uncertain, because the conversion was affected by the adsorption and desorption of NO_x during the temperature ramp, especially below 350 °C. Due to the temperature limitations of the DRIFTS cell, we carried out step-response experiments at a gas temperature of 475 °C, where the NO_x conversion was 7%.

3.2. DRIFTS experiments

Fig. 2 shows the evolution of the adsorption bands in the DRIFTS spectra obtained in the step-response experiment at 475 °C. In step 1, nitrogen oxide and oxygen ($NO + O_2$) were introduced to the system. This caused the formation of a broad band at 1556 cm^{-1} and two smaller bands at 1300 and 1245 cm^{-1}. According to the literature, the band at 1245 cm^{-1} is ascribed to monodentate nitrates on Ag/Al_2O_3 [19–21]; the band at 1300 cm^{-1}, to bidentate nitrates [19–21]; and the band at 1556 cm^{-1}, to unresolved bands of monodentate and bidentate nitrates [19–21]. Possible nitrites with bands between 1230 and 1236 cm^{-1} and at 1330 cm^{-1} [19,22] could not be distinguished, due to overlap with the bands at 1245 and 1300 cm^{-1}.

In step 2, when propene was also added ($NO + C_3H_6 + O_2$), the two nitrate bands at 1245 and 1300 cm^{-1} remained. In addition, several new bands appeared in the region between 1645 and 1377 cm^{-1}, overlapping with the nitrate bands at 1556 cm^{-1}. Bands at 1377 and 1392 cm^{-1} are assigned to adsorbed formate species according to the literature [2,21,23], whereas the band at 1392 cm^{-1} is also attributed to acetate species [8]. Bands at 1458 and 1576 cm^{-1} are assigned to carboxylate groups, which can be acetate species or free carboxylate species [2,14,15,21,23,24], and bands in the region around 1645 cm^{-1} are assigned to acrylate species [21,23,25]. Acrylate species also give rise to bands at 1570, 1455, 1378–1392, and 1297 cm^{-1} [25]. All of these bands were observed in the present study, supporting this assignment of the band at 1645 cm^{-1}.

When NO was switched off in step 3 ($C_3H_6 + O_2$), the nitrate band at 1245 cm^{-1} decreased, whereas the band at 1300 cm^{-1} increased. The increase in the latter band may be due either to an increased amount of bidentate nitrates or to the formation of another type of species. Because NO was switched off, it is more likely that the increase is due to the formation of C-containing species. Shimizu et al. ascribed a band between 1300 and 1336 cm^{-1} to carbonate species [2], and Martinez-Arias et al. attributed a band at 1298 cm^{-1} to acrylate species [23]. In parallel, a small band evolved at 2232 cm^{-1}, as shown in more detail in Fig. 3. According to the literature, bands in this region correspond to different isocyanate species. Bands between 2230 and 2235 cm^{-1} are traditionally assigned to isocyanate on Ag^+ ions [19]. More recently, Bion et al. [26] reported that isocyanate on Ag^+ absorbs at 2204 cm^{-1}, whereas the band at 2229 cm^{-1} corresponds to isocyanate on Al^{3+}. This finding

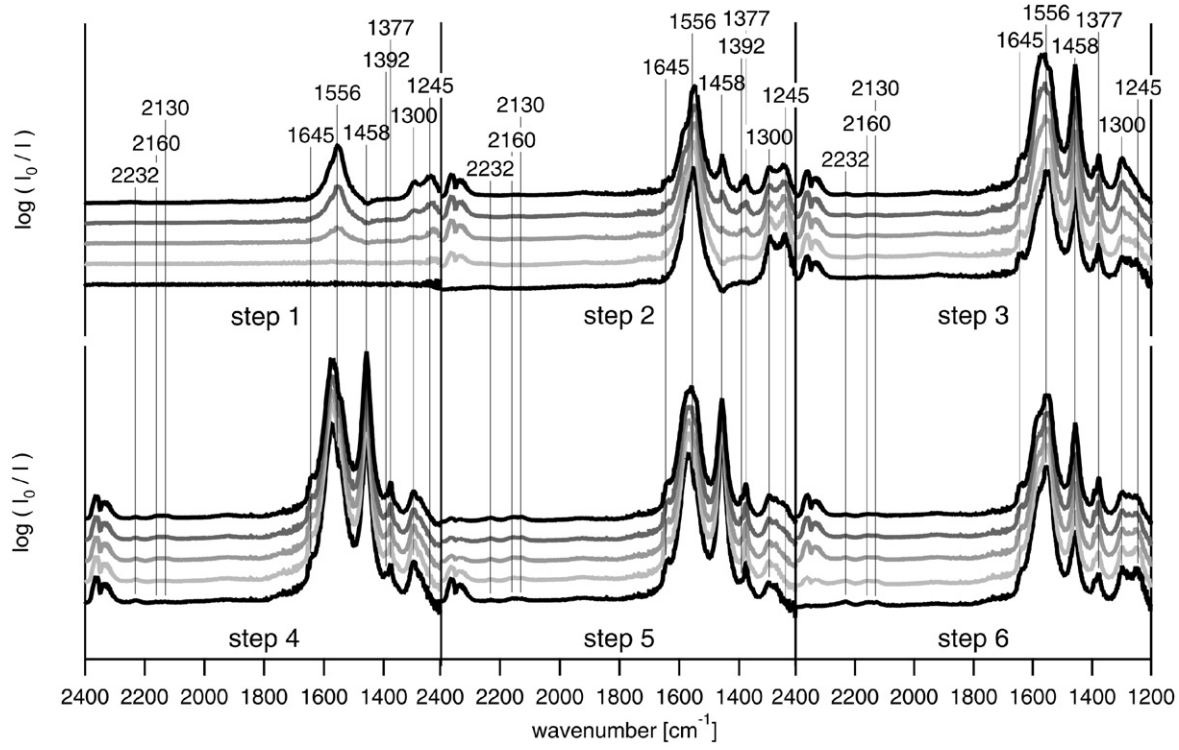

Fig. 2. Step-response experiment over the Ag/Al_2O_3 catalyst at 475 °C in a DRIFTS cell. Black line (lowermost): direct after switch in gas composition, light gray to black (uppermost): 1, 5, 10, and 15 min after switch, respectively. Gas composition for step 1: NO and O_2; step 2: NO, C_3H_6, and O_2; step 3: C_3H_6 and O_2; step 4: NO, C_3H_6, and O_2; step 5: NO and O_2; step 6: NO, C_3H_6, and O_2. Contents: 1000 ppm NO, 1000 ppm C_3H_6, 8% O_2, balance Ar.

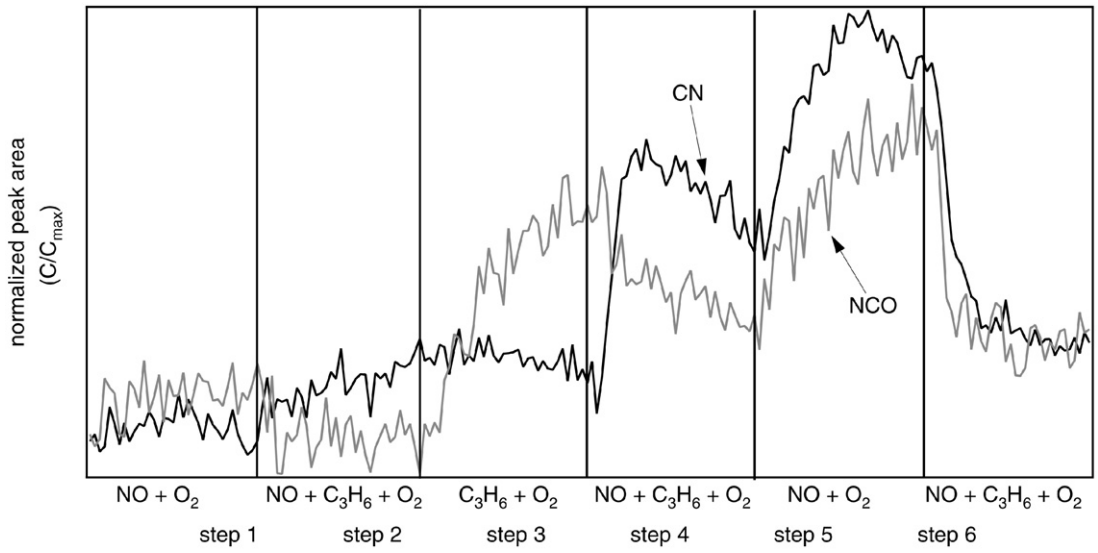

Fig. 3. Evolution of –NCO (2232 cm^{-1}) and –CN (2130 and 2160 cm^{-1}) species on the Ag/Al_2O_3 catalyst surface in the DRIFTS experiments. Gas composition for step 1: NO and O_2; step 2: NO, C_3H_6, and O_2; step 3: C_3H_6 and O_2; step 4: NO, C_3H_6, and O_2; step 5: NO and O_2; step 6: NO, C_3H_6, and O_2. Contents: 1000 ppm NO, 1000 ppm C_3H_6, 8% O_2, balance Ar.

is in accordance with the theoretical calculations of Gau and He [27].

When NO was switched on again in step 4 ($NO + C_3H_6 + O_2$), the band at 1300 cm^{-1} decreased again. The band corresponding to –NCO (2232 cm^{-1}) decreased, whereas two small and overlapping bands at 2130 and 2160 cm^{-1} increased sharply at the start of the step then decreased toward the end of the step, as shown in Fig. 3. In the literature, bands between 2127 and 2167 cm^{-1} have been assigned to cyanide (–CN) species adsorbed on the catalyst surface [19,21,23,26].

When propene was switched off in step 5 ($NO + O_2$), the bands between 1645 and 1377 cm^{-1} (mainly C-containing species, as discussed above) decreased, whereas the band at 1245 cm^{-1} (monodentate nitrate) increased (Fig. 2). The band at 1300 cm^{-1} (bidentate nitrates) also increased, albeit at a slower rate than the monodentate nitrate band. Both –NCO

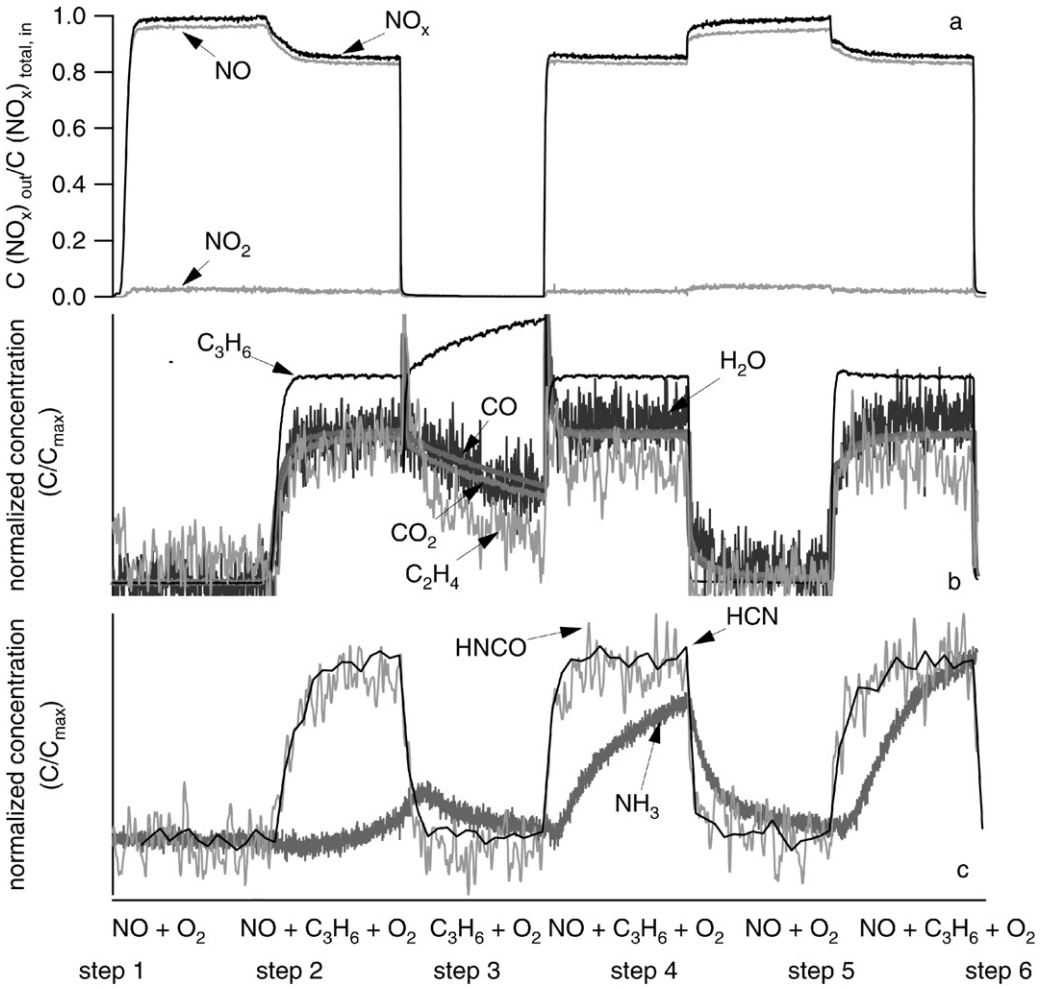

Fig. 4. Step-response experiment over the Ag/Al_2O_3 catalyst at 475 °C in the monolith reactor. Gas composition for step 1: NO and O_2; step 2: NO, C_3H_6, and O_2; step 3: C_3H_6 and O_2; step 4: NO, C_3H_6, and O_2; step 5: NO and O_2; step 6: NO, C_3H_6, and O_2. Contents: 1000 ppm NO, 500 ppm C_3H_6, 8% O_2, balance Ar. (a) Gases measured by chemiluminescence, (b and c) gases measured by gas-phase FTIR.

(2232 cm^{-1}) and –CN (2130 and 2160 cm^{-1}) increased considerably, as shown in Fig. 3. When propene was switched on again in step 6 ($NO + C_3H_6 + O_2$) the bands between 1645 and 1377 cm^{-1}, attributed to several C-containing species, increased (Fig. 2). The bands at 1300 and 1245 cm^{-1} (nitrates) started at a higher level than at the end of step 5, but decreased during the course of step 6; once more, the band at 1245 cm^{-1} decreased more than the band at 1300 cm^{-1}. Both –NCO (2232 cm^{-1}) and –CN (2130 and 2160 cm^{-1}) decreased considerably, as shown in Fig. 3.

3.3. Step response experiments in the flow reactor

We performed the same step response experiment in the flow reactor as was conducted in the DRIFTS cell. The evolution of the concentrations of several gases during the different steps is plotted in Fig. 4. The concentrations of NO, NO_2, and total NO_x are shown in Fig. 4a, normalized with the inlet NO_x concentration. In steps 2, 4, and 6, when all gases were present ($NO + C_3H_6 + O_2$), a 17% NO_x conversion was observed. This value is somewhat higher than that seen during the temperature ramp, likely because steady-state conditions were not reached during the ramp. Without propene (steps 1 and 5), no NO_x conversion was observed, but roughly 4% of NO was oxidized to NO_2. Fig. 4b shows the changes in normalized concentrations of C-containing species and water. (The normalized concentrations were calculated from the concentration at a certain time divided by the maximum concentration measured by gas-phase FTIR during the entire measurement time in all steps.) With all gases present (NO, C_3H_6, and O_2; steps 2, 4, and 6), a reproducible amount of propene was oxidized to CO_2 and CO. When NO was switched off in step 3, the propene concentration slowly increased while the CO, CO_2, and water concentrations decreased. When propene was switched off (step 5) and then switched on again (step 6), the propene concentration reached stable values faster than the CO_2, CO, and water concentrations. Fig. 4c shows normalized concentrations of HCN, HNCO, and NH_3 for the flow reactor step-response experiments. For all six steps, the normalized concentrations of HCN and HNCO appear closely related. With all gases present (NO, C_3H_6, and O_2; steps 2, 4, and 6), the HCN and the HNCO signals increased rapidly, they dropped when either NO or propene was switched off (steps 3 and 5). The NH_3 concentration changed in a similar

way as the HCN and HNCO concentrations during the different steps, but at a much slower rate.

4. Discussion

As outlined in the Introduction, isocyanates (–NCO) and cyanide (–CN) species have been widely studied as intermediates in HC-SCR over Ag/Al_2O_3 catalysts [1–5,8,13–15,28]. In this study, we followed the accumulation of surface –NCO and –CN as a function of different feed gases and the effect of preceding feed gas composition in step-response experiments. We found that –NCO species accumulated on the surface in steps 3 and 5 when either NO or propene was switched off, following a step with all of the reactants present (see Fig. 3). Switching back to NO_x reducing conditions (i.e., all components present; steps 4 and 6) decreased the amount of –NCO species on the surface, indicating that the –NCO species were consumed more rapidly than they were formed under NO_x reduction. In contrast, when either NO or propene was absent in the feed, the consumption of –NCO species was slower than their formation, resulting in an accumulation of –NCO species on the surface. Moreover, the concentration of NH_3 in the gas phase increased under NO_x reducing conditions in steps 2, 4, and 6 (NO, C_3H_6, and O_2) and decreased when either NO or propene was switched off (see Fig. 4c). Several groups have reported NH_3 formation as a product of the fast reaction between –NCO and water [9,13,29]. When propene was switched off (step 5), no more water was formed through propene oxidation, inhibiting the formation of NH_3; however, some C-containing species remained on the surface (Fig. 2, step 5), which could continue to react with N-containing species and form –NCO. Shimizu et al. [2] and Kameoka et al. [3], studying the consumption of –NCO species, found that preadsorbed –NCO and –CN species were consumed in a flow of O_2 or a mixture of $NO + O_2$ accompanied by N_2 formation. Given this finding, our results thus indicate that the reaction between –NCO and O_2 or a mixture of $NO + O_2$ in the concentrations used in our experiments was slower than the –NCO formation, as demonstrated by the buildup of –NCO on the catalyst surface with O_2 in step 3 and the mixture of $NO + O_2$ present in the feed gas in step 5. Furthermore, –NCO formation seems to be slower than the reaction between –NCO and water, because the surface –NCO concentration decreased in steps 4 and 6.

When NO was switched off in step 3 ($C_3H_6 + O_2$), –NCO species accumulated on the surface (Fig. 3). Following our earlier reasoning, we would not expect an accumulation of –NCO as long as propene was present in the feed, because water is formed during its oxidation. Apparently, the water on the catalyst surface decreased anyway, leading to diminished –NCO consumption. This hypothesis is supported by the decreased CO, CO_2, and water concentration in the gas phase and the increased propene concentration in step 3, indicating an overall decrease in propene combustion. Summarizing the conditions under which –NCO accumulates on the catalyst surface, we can conclude that –NCO can be formed from stored surface N-containing species (probably nitrates) and stored surface C-containing species.

In the formation of C-containing surface species, activated oxygen species are believed to activate the hydrocarbon [30,31]. In more detail, Iglesias-Juez et al. have suggested that propene is activated in presence of O_2 at the methyl end, resulting in adsorbed acrylate with retention of the C=C bond [25]. Moreover, they have proposed that acrylate species continue reacting with the acid–base centers of the alumina surface, leading to acetaldehyde and formaldehyde, which subsequently react with activated NO_x species [25]. In contrast, Shimizu et al. have investigated acetates as the main C-containing precursor for –NCO formation [2] and have claimed that acetate formation from propane is a very slow step in propane-SCR [31]. The fact that the band for acetate at 1458 cm^{-1} decreased significantly in step 5 suggests that acetates may be an important C-containing intermediate for –NCO in the present study as well; however, the main C-containing intermediates in propene-SCR (i.e., acetate, acrylate, or both) cannot be determined based on our results.

The formation of –NCO species during the reaction of NO and CO over different supported and unsupported oxide catalysts has been reported previously. For the reaction of NO and CO, it is believed that NO dissociates, followed by a reaction with CO to –NCO [10–12]. For HC-SCR, however, it has been shown that –NCO is formed during the decomposition of nitromethane and nitroethane [7,9,14]. Zuzaniuk et al. suggested, moreover, that HNCO is formed from nitromethane via formohydroxamic acid (CHO–N(H)OH) [13].

Given these findings, the accumulation and consumption of surface –NCO species during the different steps shown in Fig. 3 can be explained as follows. No –NCO species were formed in step 1, because no C-containing species were available. In step 2, a sharp increase in gas-phase HNCO occurred, as shown in Fig. 4c. Due to the existence of gas-phase HNCO, a higher turnover frequency of surface –NCO species can be expected in step 2 compared with that in step 3. But no surface –NCO species where observed during the 15 min of step 2, because these species were consumed very quickly and did not accumulate. In step 3, when NO was switched off, the gas-phase HNCO concentration dropped, whereas surface –NCO species began to accumulate. Here the consumption of –NCO species slowed dramatically as the water content on the catalyst surface decreased, allowing an accumulation of surface –NCO species. Under NO_x-reducing conditions in step 4, the amount of –NCO species on the catalyst surface slowly decreased as the consumption of surface –NCO species became somewhat faster than its formation. In step 5, when NO was switched off, the –NCO species accumulated on the surface again, due to slowed consumption. This accumulation was most likely due to lack of water on the catalyst surface, similar to the situation in step 3. In step 6, the amount of –NCO species on the catalyst surface decreased for the same reason as in step 4 (i.e., faster consumption than formation). The –NCO band decreased faster in step 6 than in step 4 (see Fig. 3), likely due to differences in adsorbed surface species during the preceding step; preadsorbed nitrates on the surface and a reduced amount of C-containing species

facilitate the oxidation of new hydrocarbons and thus the formation of water. This formation of extra water may explain the faster decrease of the surface –NCO species in step 6 compared with that in step 4.

Isocyanate and cyanide species are often mentioned together in the literature, because they seem to be correlated in the reaction mechanism. In accordance with this correlation, we observed exactly the same pattern for the corresponding gas-phase species HNCO and HCN in the step-response experiments, as shown in Fig. 4c. Gas-phase HNCO and HCN were detected in all of the steps with all of the gases (NO, C_3H_6, and O_2) present, when NO reduction occurred. But when either NO or propene was switched off, the HNCO and HCN concentrations dropped immediately. Eränen et al., who reported the importance of gas-phase reactions after Ag/Al_2O_3 catalysts, studied the activity of R–NCO and R–CN for NO_x reduction and found that these species were involved in the gas-phase reaction [32,33]. Assuming that the amount of gas-phase species is correlated with the amount of reacting surface species, this suggests that surface –NCO and –CN species are involved in a similar way in NO reduction. But the accumulation and consumption of these surface species during the step response experiment did not follow the same pattern, as shown in Fig. 3.

Compared with the role of –NCO species, the role of –CN species is less clear. Preadsorbed –CN species are known to be more stable on alumina at higher temperatures compared with preadsorbed –NCO species [6,13]. Several groups have reported that –CN species react with water, yielding NH_3 and CO, or with NO_2, yielding N_2 and CO_2, over alumina and different zeolites [6,7,9]. In our experiments, we observed the most pronounced surface –CN accumulation with a feed of only NO and O_2 (step 5, Fig. 3), indicating –CN formation from stored C-containing surface compounds. In addition, the formation of gas-phase HCN and the accumulation of –CN surface species were observed only with NO present in the gas phase (see Figs. 3 and 4c). This indicates that N-containing gas-phase species (NO or NO_2) or short-lived N-containing surface species (possibly nitrites) are needed for –CN formation. Bion et al. [5] proposed that –CN is a precursor for –NCO; this proposal implies a chain of reactions,

$$\xrightarrow{a} \text{–CN} \xrightarrow{b} \text{–NCO} \xrightarrow{c} . \quad (1)$$

Cyanide species are formed by reaction(s) "a," whereas the reaction(s) consuming –CN species and forming –NCO species are summarized as "b," and those consuming –NCO species are summarized as "c." Under NO_x-reducing conditions (steps 2, 4, and 6 in Fig. 3) the difference between –NCO consumption [reaction(s) "c"] and formation [reaction(s) "b"] likely is not large, because only a slow decrease in the –NCO peak was observed in step 4. At the same time, reaction(s) "b" cannot be considerably slower than reaction(s) "a," because no substantial accumulation of –CN species occurred in step 2. If –CN were the main precursor for –NCO species, then an increase in the –CN peak should be followed by an increase in the –NCO peak. The sharp increase in the –CN peak in the beginning of step 4 (Fig. 3) was not accompanied by a subsequent increase in the –NCO peak, indicating that –CN was not the main precursor for –NCO formation under the NO_x-reducing conditions in the present study.

Formation of –CN from surface formate species and gas-phase NH_3 has been proposed by Zuzaniuk et al. based on their study of (H_3C–NO_2) as a possible intermediate in –NCO and –CN formation [13]. This pathway is not obvious in our study, in which gas-phase HCN was detected much earlier and at a different concentration trace than NH_3 in the gas phase during NO_x reduction (i.e., steps 2, 4, and 6 in Fig. 4c), although we cannot unambiguously exclude –CN formation from gas-phase NH_3 due to the possibility of readsorption of gas-phase species. Zuzaniuk et al. [13] also suggested a reaction pathway for –CN formation in which water plays an important role. Given that we found the major surface –CN accumulation in step 5 ($NO + O_2$, Fig. 3) with no water present, water does not seem to be involved in the major route for –CN formation in our study. Zuzaniuk et al. proposed oximes as a precursor for –CN formation [13]. Surface –CN formation from oximes was also proposed by Bion et al. [5], who also suggested nitroso compounds as precursor for oximes in ethanol-SCR over Ag/Al_2O_3. Cant and Liu [7] studied the decomposition of formamide (NH_2–CHO) as an alternative for nitroso methane (CH_3–NO) in excess oxygen over a Co-MFI catalyst and found that HCN was the main gas-phase product, supporting the proposition that –CN is formed from nitroso compounds.

Given these findings, the behavior of the surface –CN species during the different steps in Fig. 3 can be explained as follows. No –CN formation occurred in step 1, because no C-containing species was present in the system. In step 2, no clear accumulation of surface –CN species was observed either, because these species were readily consumed. Based on the HCN concentration in the gas phase, however, a high turnover frequency of surface –CN species could be expected. In step 3, no –CN species were formed, because no NO was present in the gas phase. The band of surface –CN species increased sharply at the start of step 4, probably due to the large amount of preadsorbed C-containing species, which reacted with either short-lived N-containing surface species or gas-phase NO_x. When these stored C-containing surface species were depleted, formation of the –CN species slowed to the point at which their consumption exceeded their formation, resulting in a decrease in the –CN band, as was seen toward the end of step 4. In the first part of step 5, the surface –CN band increased again, which can be explained by the drastic decrease in –CN consumption due to a lack of water. At the same time, C-containing surface species remained, allowing continued formation of –CN species. At the end of step 5, this type of C-containing surface species was depleted, and the consumption of –CN species was faster than its formation, resulting in a decrease in the –CN band. These findings suggest that acetate and formate were not involved as the main precursors for –CN formation, because the bands of acetate and formate remained present at the end of step 5. In the beginning of step 6, the –CN band decreased rapidly, due to rapid consumption during NO_x reduction.

Based on our findings, we propose the reaction mechanism shown in Scheme 1. Nitrogen oxide and oxygen react

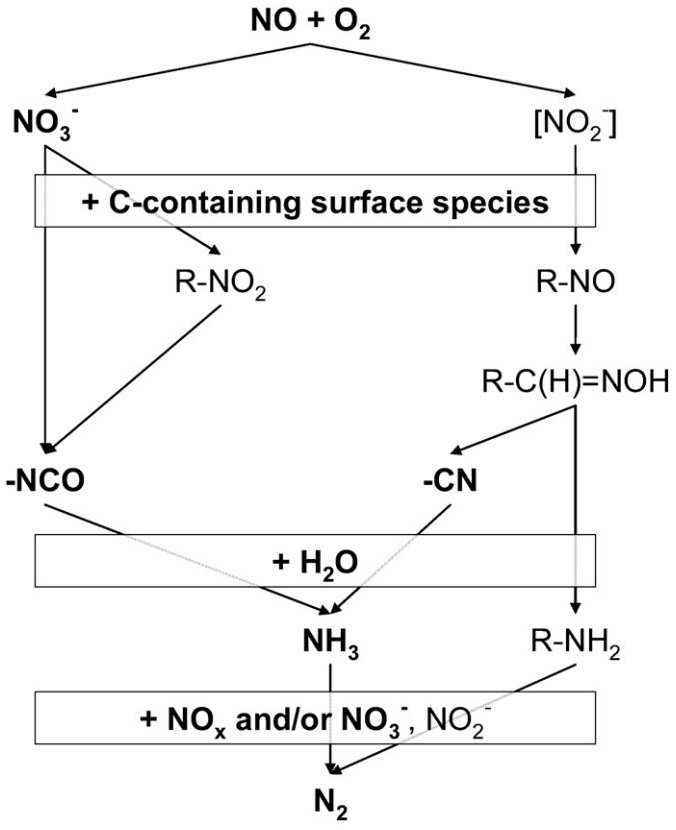

Scheme 1. Proposed reaction scheme for NO reduction in propene-SCR over Ag/Al_2O_3 catalyst. Organo-nitroso species form either with nitrites or directly with gas-phase NO_x.

and form surface nitrates and perhaps surface nitrites, even though the latter was not clearly observed in our study. Propene also reacts with oxygen and forms mainly surface formate and acetate. The reaction of surface nitrates with surface C-containing compounds, possibly acetate, leads either directly to isocyanates (–NCO) or to an organo-nitro compound (R–NO_2). The –NCO species are hydrolyzed in the presence of water to ammonia, which reacts with gas-phase NO_x or surface nitrates (and nitrites) to N_2. Similarly, surface C-containing compounds react with short-lived N-containing surface species (possibly surface nitrites) or with gas-phase NO_x to an organo-nitroso compound (R–NO), such as nitrosomethane. Nitrosomethane converts to its more stable tautomer, the oxime (R–C(H)=NOH) [7]. Oximes in turn may be reduced to amines [7,34]. Consequently, we propose that in the main route, oximes react directly to amines and/or ammonia in the presence of water, because Eränen et al. [32] found that oximes are more active for NO reduction than cyanides. In a minor route, oximes form cyanides, which react with water and form ammonia. The formation of –NCO and –CN in two parallel reaction pathways is in accordance with the findings of Nanba et al. [9], who studied the formation of –NCO from nitroethylene and expected a similar pathway via nitrosoethylene for –CN formation.

In our proposed reaction scheme, the presence of water is crucial in both paths for the formation of amines and/or ammonia, which are the final steps before N_2 formation, explaining why water on the catalyst surface is necessary for N_2 formation. Water has been reported to inhibit the nonselective oxidation of octane [35], and less propene is needed to achieve 50% NO_x conversion in the presence of water than without water [36]. Moreover, a loss of activity on the introduction of water has been reported for propene-SCR, explained by competing adsorption between propene and water [36]. For NO, it was reported that NO did not adsorb on Ag/Al_2O_3 in a gas stream of NO, O_2, and 12% water below 400 °C, in contrast to the results of experiments without water; however, in the presence of NO, NO_2, and water, silver nitrate and aluminum nitrate were already formed at 150 °C [37].

Consequently, in our proposed reaction scheme, the presence of larger amounts of water most likely will affect different steps; it will retard the formation of C-containing surface species and nitrates through competition of adsorption sites and accelerate the formation of NH_3 from –NCO and –CN, thereby increasing the overall NO_x reduction selectivity. A detailed description of how water influences the balance between the two proposed parallel reaction paths awaits further study, however.

5. Conclusion

We carried out step-response experiments under similar conditions by in-situ DRIFTS and in a flow reactor. Isocyanate and cyanide surface species showed different traces during the step-response experiments compared with the corresponding gas-phase species HNCO and HCN, which were always detected at the same time. Based on the correlation of these species, we propose a reaction mechanism involving two parallel reaction pathways for isocyanate (–NCO) and cyanide (–CN) species. Isocyanates, the intermediates of one pathway, are formed in a surface reaction between nitrates and C-containing compounds, which react either directly to –NCO or via an organo-nitro compound. Isocyanates are hydrolyzed, forming ammonia, which reacts with gas-phase NO_x or surface nitrates (and nitrites) to N_2. In the other pathway, surface C-containing compounds react with short-lived N-containing surface species (possibly nitrites) or gas-phase NO_x to organo-nitroso compounds. These are converted to their more stable tautomers, the oximes. Oximes form mainly amines and, to a minor degree, cyanides, which react with water and form ammonia, which leads to N_2 formation.

Acknowledgments

This work was performed within the EMFO Program, which is funded by the Swedish Agency for Innovation Systems, the Swedish Road Administration, and the Swedish Environmental Protection Agency, and was carried out at the Competence Centre for Catalysis, which is supported by the Swedish Energy Agency, AB Volvo, Volvo Car Corporation, Scania CV AB, GM Powertrain Sweden AB, Haldor Topsøe A/S, and the Swedish Space Corporation. Financial support from Knut and Alice Wallenberg Foundation, Dnr KAW 2005.0055, is gratefully acknowledged. The authors thank Dr. Miroslawa Abul-Milh and Dr. Jazaer Dawody for fruitful discussions.

References

[1] R. Burch, J.P. Breen, F.C. Meunier, Appl. Catal. B 39 (2002) 283.
[2] K. Shimizu, J. Shibata, H. Yoshida, A. Satsuma, T. Hattori, Appl. Catal. B 30 (2001) 151.
[3] S. Kameoka, T. Chafik, Y. Ukisu, T. Miyadera, Catal. Lett. 55 (1998) 211.
[4] S. Sumiya, H. He, A. Abe, N. Takezawa, K. Yoshida, J. Chem. Soc. Faraday Trans. 94 (1998) 2217.
[5] N. Bion, J. Saussey, M. Haneda, M. Daturi, J. Catal. 217 (2003) 47.
[6] A. Obuchi, C. Wögerbauer, R. Köppel, A. Baiker, Appl. Catal. A 19 (1998) 9.
[7] N.W. Cant, I.O.Y. Liu, Catal. Today 63 (2000) 133.
[8] X.L. Zhang, H. He, Z.C. Ma, Chem. Commun. 8 (2007) 187.
[9] T. Nanba, A. Obuchi, Y. Sugiura, C. Kouno, J. Uchisawa, S. Kushiyama, J. Catal. 211 (2002) 53.
[10] J. Rasko, F. Solymosi, J. Chem. Soc. Faraday Trans. I 76 (1980) 2383.
[11] W.C. Hecker, A.T. Bell, J. Catal. 85 (1984) 389.
[12] F. Solymosi, J. Rasko, J. Catal. 63 (1980) 217.
[13] V. Zuzaniuk, F.C. Meunier, J.R.H. Ross, J. Catal. 202 (2001) 340.
[14] F.C. Meunier, V. Zuzaniuk, J.P. Breen, M. Olsson, J.R.H. Ross, Catal. Today 59 (2000) 287.
[15] H. He, Y.B. Yu, Catal. Today 100 (2005) 37.
[16] M. Andersson, J.S. Pedersen, A.E.C. Palmqvist, Langmuir 21 (2005) 11387.
[17] H.H. Ingelsten, J.C. Beziat, K. Bergkvist, A. Palmiqvist, M. Skoglundh, Q.H. Hu, L.K.L. Falk, K. Holmberg, Langmuir 18 (2002) 1811.
[18] J. Dawody, M. Skoglundh, S. Wall, E. Fridell, J. Mol. Catal. A 225 (2005) 259.
[19] K.I. Hadjiivanov, Catal. Rev. Sci. Eng. 42 (2000) 71.
[20] S. Kameoka, Y. Ukisu, T. Miyadera, Phys. Chem. Chem. Phys. 2 (2000) 367.
[21] B. Wichterlová, P. Sazama, J.P. Breen, R. Burch, C.J. Hill, L. Čapek, Z. Sobalík, J. Catal. 235 (2005) 195.
[22] F.C. Meunier, J.P. Breen, V. Zuzaniuk, M. Olsson, J.R.H. Ross, J. Catal. 187 (1999) 493.
[23] A. Martinez-Arias, M. Fernandez-Garcia, A. Iglesias-Juez, J.A. Anderson, J.C. Conesa, J. Soria, Appl. Catal. B 28 (2000) 29.
[24] P. Sazama, L. Capek, H. Drobna, Z. Sobalik, J. Dedecek, K. Arve, B. Wichterlová, J. Catal. 232 (2005) 302.
[25] A. Iglesias-Juez, A.B. Hungria, A. Martinez-Arias, A. Fuerte, M. Fernandez-Garcia, J.A. Anderson, J.C. Conesa, J. Soria, J. Catal. 217 (2003) 310.
[26] N. Bion, J. Saussey, C. Hedouin, T. Seguelong, M. Daturi, Phys. Chem. Chem. Phys. 3 (2001) 4811.
[27] H.W. Gao, H. He, Spectrochim. Acta A 61 (2005) 1233.
[28] S. Kameoka, T. Chafik, Y. Ukisu, T. Miyadera, Catal. Lett. 51 (1998) 11.
[29] H.H. Ingelsten, M. Skoglundh, Catal. Lett. 106 (2006) 15.
[30] K. Shimizu, J. Shibata, A. Satsuma, J. Catal. 239 (2006) 402.
[31] J. Shibata, K. Shimizu, S. Satokawa, A. Satsuma, T. Hattori, Phys. Chem. Chem. Phys. 5 (2003) 2154.
[32] K. Eränen, L.E. Lindfors, F. Klingstedt, D.Y. Murzin, J. Catal. 219 (2003) 25.
[33] K. Eränen, F. Klingstedt, K. Arve, L.E. Lindfors, D.Y. Murzin, J. Catal. 227 (2004) 328.
[34] Oximes, Micropædia, in: Encyclopædia Britannica, 2007, p. 34.
[35] K. Shimizu, A. Satsuma, T. Hattori, Appl. Catal. B 25 (2000) 239.
[36] F.C. Meunier, R. Ukropec, C. Stapleton, J.R.H. Ross, Appl. Catal. B 30 (2001) 163.
[37] R. Brosius, K. Arve, M.H. Groothaert, J.A. Martens, J. Catal. 231 (2005) 344.